

Optimal control of nonlinear systems with unsymmetrical input constraints and its application to the UAV circumnavigation problem

Yangguang Yu, Xiangke Wang, *Senior Member, IEEE*, Zhiyong Sun, *Member, IEEE*, and Lincheng Shen

Abstract—In this paper, a novel design scheme is introduced to solve the optimal control problem for nonlinear systems with unsymmetrical and state-dependent input constraints. By introducing an initial stabilizing control policy as the baseline of the constructed optimal control policy, we remove the assumption in the current study for the adaptive optimal control, that is, the internal dynamics should hold zero when the state of the system is in the origin. Particularly, nonlinear control systems with partially-unknown dynamics are investigated and the procedure to acquire the corresponding optimal control policy is presented. The stability for the closed-loop dynamics and the optimality of the obtained control policy are both proved. Besides, we apply the proposed control design framework to solve the optimal circumnavigation problem based on the accumulative Fisher information for a fixed-wing unmanned aerial vehicle (UAV). The control performance of our algorithm is compared with that of the existing circumnavigation control policy in a numerical simulation.

Index Terms—Actuator saturation; Unsymmetrical constrained input system; optimal control; UAV circumnavigation; Fisher information

I. INTRODUCTION

Literature review: In the domain of automatic control, the basic requirement for the controller is to stabilize the system and drive the interested state to an equilibrium state. But when the related resource is limited or the system is required to compete for a specific performance index, the optimal behavior of the system with respect to specified long-term goals is desired. Therefore, optimal control for nonlinear systems has been the focus of the research since last century [1] as it can help improve the system performance effectively. There have been numerous successful applications of nonlinear optimal control to different fields such as spacecraft attitude control [2] and underwater vehicle control [3]. In general, the optimal control problem for nonlinear systems involves the solving of an underlying Hamilton-Jacobi-Bellman (HJB) equation [4], which is usually very difficult to solve and almost impossible to get an analytical solution directly [5]. To solve the HJB equation, the paper [6] proposed an off-line policy iteration (PI) strategy, in which a sequence of cost functions were approximated. The methods proposed in

[6] requires that the dynamics of the system is completely known. However, the dynamics of the nonlinear system is usually complex and even time-variant in some situations. As a consequence, nonlinear systems are rather difficult to be modeled accurately. For traditional model-based control design methods, the performance degradation caused by the model inaccuracy may be catastrophic.

To overcome the difficulties mentioned above, the adaptive dynamic programming (ADP) [7]–[9] method was developed. Different from the traditional model-based control design methods, the ADP method approximates the solution of the HJB equation using online data and further constructs the optimal control law adaptively with the system's dynamics being partially or completely unknown [10]–[12]. It was proved in previous studies [11], [13] that the ADP method can guarantee the ultimate uniform boundedness (UUB) of the system and thus the risk of system instability caused by the model inaccuracy can be avoided. For systems with partially-unknown dynamics, [14]–[16] proposed the integral reinforcement learning (IRL) method to approximate the solution of the HJB equation. When the dynamics of the system is completely unknown, an identifier-critic-actor-based structure is usually used. A neural network (NN) [17] or recurrent neural network [18] was utilized to fully identify the unknown system dynamics. Recently, the work [19] proposed a deterministic policy gradient adaptive dynamic programming algorithm for solving model-free optimal control problems. Although the preconditions and the proposed methods in the studies mentioned above are different, there exists one hidden assumption in common among these works, that is, the internal dynamics of the system should be zero when the state of the system is in the origin [11]–[16]. The system that satisfies this assumption is termed as the standard form (SF) system in this paper. However, this assumption is not satisfied in many nonlinear systems, which are termed as nonstandard form (NF) systems in this paper. For example, the control problems of target tracking [11] or UAV circumnavigation [20] involve with the NF system. It is still an unsolved problem on how to tackle the optimal control problem for the NF system.

Another important issue that is worth considering is the amplitude limitation on the control input. There often exists an unsymmetrical and state-dependent saturation zone for the input of the system's actuator in reality. Taking the attitude control of a vehicle or aircraft for example, the steering mechanism of a ground or aerial vehicle may partially loss effectiveness due to motor fault [21]. As a consequence, the

Y. Yu, X. Wang and L. Shen are with the College of Intelligence Science and Technology, National University of Defense Technology, Changsha, 410073, China (e-mail: yuyanguang11@nudt.edu.cn; xkwang@nudt.edu.cn; lcshen@sina.com).

Z. Sun is with the Department of Electrical Engineering, Eindhoven University of Technology, Eindhoven, 5600 MB, Netherlands. (email: sun.zhiyong.cn@gmail.com).

vehicle's maximum steering capacity for the left direction and the right direction may be different. Meanwhile, to avoid the risk of rollover, the maximum angular velocity of the vehicle is usually required to decrease with the increment of the linear velocity. To confront the optimal control problem with symmetrical input constraints, a non-quadratic cost function was proposed in [22] and a smooth saturated controller was further constructed. Similar studies are reported in the literature therein [11], [15], [23], [24]. In these studies, the input u is constrained in a symmetrical and fixed set, i.e., u is constrained by $|u| < \lambda$ with λ being a positive constant. For the optimal control problem with unsymmetrical input constraint, the paper [25] proposed an ADP-based neuro-optimal controller for discrete-time nonlinear systems with asymmetric input saturation. More recently, the work [21] proposed an adaptive optimal control law by introducing a switching function. We notice that the switching function in [21] should be carefully selected to guarantee the stability of the closed-loop system. The event-triggered adaptive optimal control problem was studied in [26] and [27] for a class of asymmetrically input-constrained nonlinear systems. The work [28] constructed an optimal neurocontroller under the framework of RL and the work [29] presented an event-driven H_∞ controller for continuous nonlinear systems with asymmetric input saturation. However, the work [26]–[29] can only guarantee the UUB of the closed-loop system theoretically. In summary, the proposed methods in the existing studies still exist some shortcomings. Meanwhile, none of these works mentioned above considered the adaptive optimal control problem with state-dependent input constraint.

To demonstrate the application value of the method proposed in this paper, we apply the proposed algorithm to solve the optimal UAV circumnavigation control problem, which is another main contribution of this paper. Although there have been numerous applications of UAV, the surveillance and tracking of moving ground targets is still one of the most important applications of UAV [30]. To monitor a ground target circumnavigate around the ground target with a preset radius [31]. For robots with single-integrator dynamics, different control algorithms have been proposed to achieve the circumnavigation with distance measurements [32] or bearing measurements [33]. For a non-holonomic agent, [34] proposed a circumnavigation control method while the position of the target is assumed to be unknown. Assuming the relative position of the target is accessible, the paper [20] designed a guidance law by exploiting the Vector Fields (VF) method. However, none of these works have considered the optimality issue of the circumnavigation control.

Statement of contributions: Aimed at solving the optimal control problem for nonlinear systems with state-dependent and unsymmetrical input constraints, this paper investigates the partially-unknown system whose dynamics is in NF form and an online PI algorithm is presented in this paper. The main contributions of this paper are summarized as follows:

- 1) An online PI algorithm is proposed to address the optimal control of nonlinear systems with state-dependent and unsymmetrical input constraints. The stability and convergence of the proposed algorithm are also proved.

Compared with the existing studies, our method has the following novelties:

- Compared with the existing studies such as [11], [21]–[24], [28], this paper addresses the optimal control problem with the constraint set of the input u being state-dependent rather than being constant.
 - Compared with [26], [28], [29], the closed-loop system with the proposed algorithm is theoretically guaranteed to be asymptotically stable rather than being UUB. Moreover, the method proposed in this paper does not exist the difficulty of designing switching functions in comparison with [21].
- 2) The optimal control problem for a NF system is addressed. In the current study of the adaptive optimal control, the internal dynamics is usually required to hold zero when the state of the system is in the origin. To expand the application range of the ADP theory to systems that do not meet this condition, this paper designs a special control law which consists of the initial stabilizing control law and the neural-network-based control law.
 - 3) By exploiting the method proposed in this paper, an optimal circumnavigation control law with input saturation is proposed. To the best of our knowledge, it is the first time that the UAV optimal circumnavigation problem w.r.t. an infinite-horizon performance index is addressed.

The rest of the paper is organized as follows: Section II develops our adaptive optimal control algorithm for the nonlinear systems with state-dependent and unsymmetrical input constraints. In Section III, we apply our methods to solve the optimal UAV circumnavigation control problem and a comparison with the method proposed in [20] is illustrated. Finally, the concluding remarks are drawn in Section IV.

Notation: The vector $\mathbf{1}_n \in \mathbb{R}^n$ denotes a vector with its elements all being 1 and $\mathbf{0}_{n \times m} \in \mathbb{R}^{n \times m}$ is a zero matrix. Here we define an operator $\text{vec}(\cdot) : \mathbb{R}^{n \times n} \rightarrow \mathbb{R}^n$. For a vector $\mathbf{a} \in \mathbb{R}^n$ and a diagonal matrix $M \in \mathbb{R}^{n \times n}$, if $\mathbf{a} = \text{vec}(M)$, one has $a_i = M_{ii}, i = 1, \dots, n$, where a_i is the i -th element of the vector \mathbf{a} and M_{ii} is the i -th element on the diagonal of the matrix M .

II. THE OPTIMAL CONTROL PROBLEM FOR NF SYSTEMS WITH UNSYMMETRICAL INPUT CONSTRAINTS

A. Problem formulation

Consider the following system whose dynamics is

$$\begin{cases} \dot{x}_1(t) = f_1(x_1, x_2) + g_1(x_1, x_2)u(t), \\ \dot{x}_2(t) = f_2(x_2), \end{cases} \quad (1)$$

where $x_1 \in \mathbb{R}^{n_1}$ is the system state to be stabilized; $x_2 \in \mathbb{R}^{n_2}$ is the state which is not intended to be controlled and assumed to be bounded; the continuous functions $f_1(x_1, x_2) \in \mathbb{R}^{n_1}$ and $f_2(x_2) \in \mathbb{R}^{n_2}$ are the unknown internal dynamics of the system; $g_1(x_1, x_2) \in \mathbb{R}^{n_1 \times m}$ is the input dynamics of the system; $u(t) \in \mathbb{R}^m$ is the control input. Note that the function $f_1(x_1, x_2)$ is not necessary to be zero when $x_1 = 0$.

Denote the stack vector $x \in \mathbb{R}^n$ as $x = [x_1^\top, x_2^\top]^\top$, where $n = n_1 + n_2$. The control input $u(t)$ is constrained by the condition

$$d_i(x(t)) \leq u_i(t) \leq h_i(x(t)), \quad i = 1, \dots, m, \quad (3)$$

where $u_i(t)$ is the i -th element of $u(t)$; $d_i(x(t))$ and $h_i(x(t))$ are the known functions that determine the lower bound and the upper bound for the i -th element of $u(t)$.

Remark 1: The system described by (1) and (2) can be regarded as the general form of many widely studied systems. For example, the state x_2 can be regarded as a bounded time-varying uncertainty [35] and system (1) is to be stabilized while disturbed by x_2 . Also, the system described by (1) and (2) is commonly used in the target tracking system with x_1 being the tracking error and x_2 being the state of the target. There have been many works reported on such systems in the previous literatures, such as [11], [36].

Remark 2: In this paper, the constraint set of u is unsymmetrical and state-dependent as (3) reveals. Meanwhile, the internal dynamics $f_1(x_1, x_2)$ of system (1) does not satisfy the condition that $f(x_1, x_2) = 0$ when $x_1 = 0$, which is required in the previous studies of ADP [11]–[16], [23]. As a consequence, the methods proposed in the previous studies, such as [15], [23], are inappropriate.

The aim of this paper is to design an optimal policy $u^*(t) = \mu^*(x)$ constrained by the unsymmetrical set (3) such that the x_1 -system is stabilized as well as a performance index $\mathcal{J}(x(0), u)$ defined in the following form is minimized:

$$\mathcal{J}(x(0), u) = \int_0^\infty [Q(x_1) + U_n(u, x)] d\tau, \quad x(0) = x^o, \quad (4)$$

where $Q(x_1)$ is a positive semi-definite function related with the state x_1 , $U_n(u, x)$ is a positive semi-definite function which is to be designed, and x^o is the initial state.

Before presenting the solution to the optimal control problem described above, we firstly introduce a definition of the admissible control.

Definition 1 (Admissible Control [6]): For a given system described by (1) and (2), a control policy $u(t) = \mu(x)$ is defined to be admissible with respect to the performance index (4) on a compact set $\Omega \subseteq \mathbb{R}^n$, written as $\mu(x) \in \mathcal{A}(\Omega)$, if $\mu(x)$ is continuous, $u(t) = \mu(x)$ stabilizes system (1) and $\mathcal{J}(x^o, u)$ is finite for every $x^o \in \Omega$.

Similar to the previous works, such as [11], [14], the following assumption is set in this paper.

Assumption 1: There exists a known admissible control policy on a set $\Omega \subseteq \mathbb{R}^n$ which stabilizes system (1) and satisfies constraint (3).

Remark 3: In many scenarios of nonlinear system controls with input saturation, such as trajectory-tracking control [37] and formation control [38], some Lyapunov-based methods have been proposed to design a stabilizing but non-optimal control policy with input saturation, and thus an initial admissible control policy can be obtained. In some industrial applications, the initial admissible controller also can be constructed by empirical methods, such as tuning the control parameters of a PID controller.

B. The design method for NF systems with unsymmetrical and state-dependent input constraints

If Assumption 1 holds, the initial admissible control policy is denoted as $u_s(t) = \mu_s(x(t))$. Although the initial control policy $u_s(t)$ is stabilizing, the control performance of $u_s(t)$ may not be satisfactory. Thus, based on the initial control policy $u_s(t)$, we design the control policy $u(t)$ as

$$u(t) = u_s(t) + \hat{u}(t), \quad (5)$$

where $\hat{u}(t)$ is a to-be-designed virtual input which enables the actual control input $u(t)$ to achieve the optimal control performance. As $u(t)$ is constrained by (3), the virtual input $\hat{u}(t)$ should satisfy

$$d_i(x(t)) - u_s^i(t) \leq \hat{u}_i(t) \leq h_i(x(t)) - u_s^i(t), \quad i = 1, \dots, m, \quad (6)$$

where $\hat{u}_i(t)$ and $u_s^i(t)$ are the i -th element of $\hat{u}(t)$ and $u_s(t)$, respectively. Further by employing (5), system (1) is rewritten as

$$\dot{x}_1(t) = F_s(x_1, x_2) + g_1(x_1, x_2)\hat{u}(t), \quad (7)$$

where the function $F_s(x_1, x_2)$ is defined by

$$F_s(x_1, x_2) = f_1(x_1, x_2) + g_1(x_1, x_2)\mu_s(x).$$

Define two sets of functions $\bar{\lambda}_i(u, x)$ and $\hat{\lambda}_i(\hat{u}, x)$, $i = 1, 2, \dots, m$, as

$$\begin{aligned} \bar{\lambda}_i(u, x) &= \begin{cases} h_i(x) - \mu_s^i(x), & \text{if } u_i - \mu_s^i(x) \geq 0, \\ -d_i(x) + \mu_s^i(x), & \text{if } u_i - \mu_s^i(x) < 0, \end{cases} \\ \hat{\lambda}_i(\hat{u}, x) &= \begin{cases} h_i(x) - \mu_s^i(x), & \text{if } \hat{u}_i \geq 0, \\ -d_i(x) + \mu_s^i(x), & \text{if } \hat{u}_i < 0. \end{cases} \end{aligned} \quad (8)$$

Note that if Assumption 1 is satisfied, it holds that

$$d_i(x) < \mu_s^i(x) < h_i(x), \quad i = 1, \dots, m,$$

which yields

$$d_i(x) - \mu_s^i(x) < 0 < h_i(x) - \mu_s^i(x), \quad i = 1, \dots, m, \quad (9)$$

where $\mu_s^i(x)$ is the i -th element of the function $\mu_s(x)$. The inequality (9) guarantees that $\bar{\lambda}_i(u, x) = \hat{\lambda}_i(\hat{u}, x) \geq 0$ if $\hat{u}_i = u_i - \mu_s^i(x)$.

Inspired by the previous studies such as [11], we design the control cost function $U_n(u, x)$ for system (1) as

$$U_n(u, x) = 2 \sum_{i=1}^m \int_0^{u_i - \mu_s^i(x)} \bar{\lambda}_i r_i (\tanh^{-1}(s/\bar{\lambda}_i)) ds, \quad (10)$$

where r_i is a positive constant and $\bar{\lambda}_i \triangleq \bar{\lambda}_i(u, x)$.

Remark 4: Note that compared with the design of the previous literatures, such as [11], [15], [23], the scaling factor $\bar{\lambda}_i$ is a function related with the system state rather than a constant in order to tackle the unsymmetrical input constraint and the NF form of the system. Meanwhile, the upper bound of the integral in (10) takes the initial admissible control policy $\mu_s(x)$ into consideration, which is also different from the design of the previous studies.

The issue that remains is to design a virtual input $\hat{u}(t)$ such that the control policy $u(t)$ given by (5) is optimal w.r.t. the

performance index (4). To achieve this target, we define a performance index $\mathcal{J}_2(x(0), \hat{u})$ for system (7) as

$$\mathcal{J}_2(x(0), \hat{u}) = \int_0^\infty [Q(x_1) + \hat{U}_n(\hat{u}, x)] d\tau, \quad x(0) = x^o, \quad (11)$$

where the function $\hat{U}_n(\hat{u}, x)$ is defined by

$$\begin{aligned} \hat{U}_n(\hat{u}, x) &= 2 \sum_{i=1}^m \int_0^{\hat{u}_i} r_i \hat{\lambda}_i \left(\tanh^{-1}(s/\hat{\lambda}_i) \right) ds \\ &= 2 \sum_{i=1}^m \hat{\lambda}_i \tanh^{-1} \left(\hat{u}_i/\hat{\lambda}_i \right) r_i \hat{u}_i \\ &\quad + \sum_{i=1}^m \hat{\lambda}_i^2 r_i \ln \left(\mathbf{1}_n - \left(\hat{u}_i/\hat{\lambda}_i \right)^2 \right), \quad (12) \end{aligned}$$

and $\hat{\lambda}_i \triangleq \hat{\lambda}_i(\hat{u}, x)$. Based on the design of the functions $\bar{\lambda}_i(u, x)$, $\hat{\lambda}_i(\hat{u}, x)$, $U_n(u, x)$ and $\hat{U}_n(\hat{u}, x)$ in (8), (10) and (12), we will show how to design an optimal control law for NF systems with unsymmetrical and state-dependent input constraints in the following part.

The function $F_s(x_1, x_2)$ and the virtual input $\hat{u}(t)$ can be regarded as the internal dynamics and control input of system (7), respectively. As the initial control policy $u_s(t)$ is an admissible control of system (1), it holds that $F_s(0, x_2) = 0$. Otherwise, when $u(t) = u_s(t)$ and $x_1 = 0$, it holds that $\dot{x}_1 = F_s(0, x_2) \neq 0$, which contradicts with the fact that system (1) can be stabilized by the control policy $u_s(t)$. Moreover, since $F_s(0, x_2) = 0$, the virtual input \hat{u} should hold zero when $x_1 = 0$. As a consequence, by using (5), system (1) is transformed into system (7), which meets the requirement for the admissible control defined in Definition 1.

Remark 5: In the previous works, such as [11], [14], the initial admissible control policy $u_s(t)$ is only used in the initial policy iteration. However, in this paper, it can be observed from (5) that the initial admissible control policy $u_s(t)$ also acts as a baseline for constructing the optimal control law. Then the to-be-designed virtual input $\hat{u}(t)$ is added on the initial control policy $u_s(t)$ to obtain an optimized control performance. By this method, the internal dynamics $f_1(x_1, x_2)$ of system (1) is not necessary to be zero when $x_1 = 0$.

The following lemma shows that the optimal control problem for system (1) can be transformed into the optimal control problem for system (7).

Lemma 1: Given a unique optimal control policy $\hat{u}^*(t)$ for system (7) w.r.t. the performance index (11), the control policy $u^*(t)$ given by

$$u^*(t) = \hat{u}^*(t) + u_s(t) \quad (13)$$

is the unique optimal control policy for system (1) w.r.t. the performance index (4).

Proof: Given two control policies $u(t)$ and $\hat{u}(t)$ satisfying (5) with the same initial states, the trajectories of system (1) and system (7) are identical. Meanwhile, from (8), it can be observed that $\bar{\lambda}_i(u, x) = \hat{\lambda}_i(\hat{u}, x)$. Further, from (10) and (12), it holds that $U_n(u, x) = \hat{U}_n(\hat{u}, x)$ if $u = \mu_s(x) + \hat{u}$, which further implies $\mathcal{J}(x(0), u) = \mathcal{J}_2(x(0), \hat{u})$. Suppose the control policy $u^*(t)$ given by (13) is not the unique optimal control policy, there always exists a control policy $u'(t)$ such that

$$\mathcal{J}(x(0), u') \leq \mathcal{J}(x(0), u^*). \quad (14)$$

Define a control policy $\hat{u}'(t) = u'(t) - u_s(t)$. Through the discussion above, one has

$$\mathcal{J}(x(0), u') = \mathcal{J}_2(x(0), \hat{u}'). \quad (15)$$

By using (14) and (15), it yields

$$\mathcal{J}_2(x(0), \hat{u}') = \mathcal{J}(x(0), u') \leq \mathcal{J}(x(0), u^*) = \mathcal{J}_2(x(0), \hat{u}^*),$$

which contradicts with the fact that $\hat{u}^*(t)$ is the optimal control policy. Thus, $u^*(t)$ given by (13) is the unique optimal control policy for system (1) w.r.t. the performance index (4). ■

Lemma 1 shows that the optimal control policy $u^*(t)$ for system (1) w.r.t. the performance index (4) can be obtained if the optimal control policy $\hat{u}^*(t)$ is available. Thus, we introduce the procedure of designing $\hat{u}^*(t)$ in the following part.

Using (2) and (7), the dynamics of the state x can be rewritten as

$$\dot{x} = F(x) + G(x)\hat{u}, \quad (16)$$

where

$$\begin{aligned} F(x) &= [F_s(x)^\top, f_2(x_2)^\top]^\top, \\ G(x) &= [g_1(x_1, x_2)^\top, \mathbf{0}_{n_2 \times m}^\top]^\top. \end{aligned}$$

Assume there exists a continuously differentiable value function $V^*(x)$ defined by

$$V^*(x(t)) = \min_{\hat{u} \in \mathcal{A}(\Omega)} \int_t^\infty [Q(x_1) + \hat{U}_n(\hat{u}, x)] d\tau. \quad (17)$$

A Hamiltonian function $\hat{H}(x, V^*, \hat{u})$ is defined as

$$\hat{H}(x, V^*, \hat{u}) = (V_x^*)^\top (F + G\hat{u}) + Q(x_1) + \hat{U}_n(\hat{u}, x), \quad (18)$$

where $F \triangleq F(x)$, $G \triangleq G(x)$, $V^* \triangleq V^*(x)$, and $V_x^* = \partial V^*(x)/\partial x \in \mathbb{R}^n$. Then, similar to the previous works [11], [15], [23], by using the stationarity condition (see [4]) on the Hamiltonian function $\hat{H}(x, V^*, \hat{u})$, i.e., $\partial \hat{H}/\partial \hat{u} = 0$, we obtain the optimal control policy $\hat{u}^*(t)$ as

$$\begin{aligned} \hat{u}^*(t) &= \hat{\mu}^*(x(t)) = \arg \min_{\hat{u} \in \mathcal{A}(\Omega)} \hat{H}(x, V^*, \hat{u}) \\ &= -\hat{\lambda} \tanh \left((1/2)(\hat{\lambda}R)^{-1} G^\top V_x^* \right), \end{aligned} \quad (19)$$

where $\hat{\lambda}, R \in \mathbb{R}^{m \times m}$ are diagonal matrices whose i -th elements on the diagonal are $\hat{\lambda}_i$ and r_i , respectively. It can be observed from (19) that $|\hat{u}_i| \leq \hat{\lambda}_i(\hat{u}_i, x)$, based on which the inequality (6) can be derived. Further, the control policy $u(t)$ defined by (5) can satisfy the constraint (3).

Next, substituting (19) into (12) results in

$$\begin{aligned} \hat{U}_n(\hat{u}^*, x) &= (V_x^*)^\top G \hat{\lambda} \tanh(\hat{D}^*) \\ &\quad + (\text{vec}(\hat{\lambda}R\hat{\lambda}))^\top \ln \left(\mathbf{1}_n - \tanh^2(\hat{D}^*) \right), \quad (20) \end{aligned}$$

where $\hat{D}^* = (1/2)(\hat{\lambda}R)^{-1} G^\top V_x^*$. By putting (20) and (19) into (18), it yields the following HJB equation:

$$\begin{aligned} (\text{vec}(\hat{\lambda}R\hat{\lambda}))^\top \ln \left(\mathbf{1}_n - \tanh^2(\hat{D}^*) \right) \\ + Q(x_1) + (V_x^*)^\top F(x) = 0. \quad (21) \end{aligned}$$

If the solution V_x^* of the HJB equation (21) is found, the optimal virtual input \hat{u}^* for the system (7) can be obtained by (19), and the optimal control policy $u^*(t)$ for system (1) is further obtained according to (13).

In the following theorem, it is proved that the control law $u^*(t)$ defined by (13) and (19) is the unique optimal control policy w.r.t. the performance index (4) and stabilizes the x_1 -system.

Theorem 1: Consider the optimal control problem for system (1) w.r.t. the performance index (4). Suppose that $V^*(x)$ is a positive-definite solution to the HJB equation (21). Then the control policy $u^*(t)$ defined by (13) and (19) is the unique optimal control policy such that system (1) is stabilized asymptotically and the performance index (4) is minimized.

Proof: Firstly, we will prove that $u^*(t)$ is the unique optimal policy that minimizes the performance index (4). It has been proved in Lemma 1 that the optimality of the control policy $u^*(t)$ for system (1) w.r.t. the performance index (4) is equivalent to the optimality of the control policy $\hat{u}^*(t)$ w.r.t. the performance index (11). Thus, one only needs to prove that $\hat{u}^*(t)$ is the unique optimal control policy for system (7) w.r.t. the performance index (11).

Note that for the optimal value function $V^*(x(t))$ defined by (17), one has

$$\int_0^\infty \left(\dot{V}^*(x(\tau)) \right) d\tau = -V^*(x(0)).$$

Then given an admissible control law $\hat{u}(t)$, the performance index (11) can be rewritten as

$$\begin{aligned} \mathcal{J}_2(x(0), \hat{u}) &= \int_0^\infty \left[Q(x_1) + \hat{U}_n(\hat{u}, x) \right] d\tau + V^*(x(0)) \\ &\quad + \int_0^\infty \left(\dot{V}^*(x) \right) d\tau \\ &= \int_0^\infty \left[Q(x_1) + \hat{U}_n(\hat{u}, x) \right] d\tau + V^*(x(0)) \\ &\quad + \int_0^\infty \left[(V_x^*)^\top (F + G\hat{u}^*) + (V_x^*)^\top G(\hat{u} - \hat{u}^*) \right] d\tau. \end{aligned} \quad (22)$$

By adding and subtracting the term $\hat{U}_n(\hat{u}^*, x)$ in the integral part, (22) becomes

$$\begin{aligned} \mathcal{J}_2(x(0), \hat{u}) &= V^*(x(0)) \\ &\quad + \int_0^\infty \left[\hat{U}_n(\hat{u}, x) - \hat{U}_n(\hat{u}^*, x) + (V_x^*)^\top G(\hat{u} - \hat{u}^*) \right] d\tau \\ &\quad + \int_0^\infty \left[(V_x^*)^\top (F + G\hat{u}^*) + Q(x_1) + \hat{U}_n(\hat{u}^*, x) \right] d\tau. \end{aligned} \quad (23)$$

It can be observed from (12) and (19) that

$$\begin{aligned} &\hat{U}_n(\hat{u}, x) - \hat{U}_n(\hat{u}^*, x) \\ &= 2 \sum_{i=1}^m \int_{\hat{u}_i^*}^{\hat{u}_i} r_i \hat{\lambda}_i \left(\tanh^{-1}(s/\hat{\lambda}_i) \right) ds. \\ &(V_x^*)^\top G = -2 \sum_{i=1}^m r_i \hat{\lambda}_i \tanh^{-1}(\hat{u}_i^*/\hat{\lambda}_i). \end{aligned}$$

Thus we have

$$\begin{aligned} M_u &\triangleq \hat{U}_n(\hat{u}, x) - \hat{U}_n(\hat{u}^*, x) + (V_x^*)^\top G(\hat{u} - \hat{u}^*) \\ &= 2 \sum_{i=1}^m \int_{\hat{u}_i^*}^{\hat{u}_i} r_i \hat{\lambda}_i \left(\tanh^{-1}(s/\hat{\lambda}_i) \right) ds \\ &\quad - 2 \sum_{i=1}^m r_i \hat{\lambda}_i \tanh^{-1}(\hat{u}_i^*/\hat{\lambda}_i) (\hat{u}_i - \hat{u}_i^*). \end{aligned} \quad (24)$$

Using Leibniz's rule to differentiate $V^*(x)$ along the trajectory of system $\dot{x} = F(x) + G(x)\hat{u}^*$, it yields

$$(V_x^*)^\top (F + G\hat{u}^*) = -Q(x_1) - \hat{U}_n(\hat{u}^*, x),$$

which implies

$$\hat{H}(x, V^*, \hat{u}^*) = 0. \quad (25)$$

By employing (24) and (25), (23) becomes

$$\begin{aligned} \mathcal{J}_2(x(0), \hat{u}) &= \int_0^\infty \hat{H}(x, V^*, \hat{u}^*) d\tau + \int_0^\infty M_u(\tau) d\tau \\ &\quad + V^*(x(0)) \\ &= \int_0^\infty M_u(\tau) d\tau + V^*(x(0)). \end{aligned} \quad (26)$$

To prove that $\hat{u}^*(t)$ is the unique optimal control policy, one only needs to show that $M_u > 0$ always holds for all $\hat{u} \neq \hat{u}^*$ and M_u equals zero if and only if $\hat{u} = \hat{u}^*$. Here we define a function $f_\alpha(a, b)$ as

$$f_\alpha(a, b) = \int_a^b \beta(s) ds - \beta(a)(b - a), \quad (27)$$

where $\beta(s)$ is a monotonically increasing function. It can be verified that $f_\alpha(a, b) > 0$ always holds for $\forall a \neq b$ and $f_\alpha(a, b) = 0$ when $a = b$. Let $\beta(s) = \tanh^{-1}(s/\hat{\lambda}_i)$ and for all $\hat{u} \neq \hat{u}^*$, we have

$$M_u = 2r_i \hat{\lambda}_i \sum_{i=1}^m f_\alpha(\hat{u}_i^*, \hat{u}_i) > 0.$$

Note that $V^*(x)$ is a positive semi-definite function and $V^*(x) = 0$ if and only if $\|x_1\| = 0$. As a consequence, the function $V^*(x)$ can be utilized as a Lyapunov function for x_1 . From $H(x, V^*, \hat{u}^*) = 0$, it yields

$$\begin{aligned} \frac{dV^*(x)}{dt} &= (V_x^*)^\top (F + G\hat{u}^*(x)) \\ &= -Q(x_1) - \hat{U}_n(\hat{u}, x) \leq 0. \end{aligned} \quad (28)$$

The equality in (28) holds if and only if $\|x_1\| = 0$. As a consequence, the x_1 -system is asymptotically stable. ■

C. Online policy iteration algorithm for solving the HJB-equation

To derive $\hat{u}^*(t)$ based on (19), the solution V_x^* of the HJB equation (21) has to be solved. However, since (21) is usually highly nonlinear, it is quite difficult to get its analytical solution. In the following part, to obtain an equivalent formulation of HJB which does not need the knowledge of the internal dynamics $f_1(x_1, x_2)$ and $f_2(x_2)$, the IRL idea introduced in [16] is employed.

Let $T > 0$ denote the integral reinforcement interval and it holds that

$$V(x(t)) = \int_t^{t+T} [Q(x_1) + \hat{U}_n(\hat{u}, x)] d\tau + V(x(t+T)). \quad (29)$$

Based on (29), the following IRL-based PI algorithm is utilized to get the solution of the HJB equation (21) with the internal dynamics $f_1(x_1, x_2)$ and $f_2(x_2)$ unknown.

1. (Policy evaluation) given an admissible control policy $\hat{\mu}^{(k)}(x)$, update $V^{(k)}(x)$ by the Bellman equation

$$V^{(k)}(x(t)) = \int_t^{t+T} [Q(x_1) + \hat{U}_n(\hat{u}, x)] d\tau + V^{(k)}(x(t+T)). \quad (30)$$

2. (Policy improvement) update the control policy according to

$$\hat{\mu}^{(k+1)}(x) = -\hat{\lambda} \tanh \left((1/2)(\hat{\lambda}R)^{-1} G^\top(x) V_x^{(k)} \right), \quad (31)$$

where $V_x^{(k)} \triangleq \partial V^{(k)}(x)/\partial x$; the notations $V^{(k)}(x)$ and $\hat{\mu}^{(k)}(x)$ represent the value function and the virtual control policy in the k -th iteration, respectively.

The following theorem shows that the IRL method introduced above can be employed to improve the control law.

Theorem 2: Let $\hat{u}^{(k)} = \hat{\mu}^{(k)}(x) \in \mathcal{A}(\Omega)$ and $V^{(k)}(x)$ satisfy $H(x, V^{(k)}, \hat{u}^{(k)}) = 0$ with the boundary condition $V^{(k)}(0) = 0$. Then, the control policy $\hat{\mu}^{(k+1)}(x)$ defined by (31) is an admissible control for system (7). Moreover, if $V^{(k+1)}(x)$ is the positive semi-definite function that satisfies $H(x, V^{(k+1)}, \hat{u}^{(k+1)}) = 0$ with $V^{(k+1)}(0) = 0$, it holds that $V^*(x) \leq V^{(k+1)}(x) \leq V^{(k)}(x)$.

Proof: We first prove that $\hat{u}^{(k+1)} \in \mathcal{A}(\Omega)$. Taking the derivative of $V^{(k)}(x)$ along the trajectory of system $\dot{x} = F(x) + G(x)\hat{u}^{(k+1)}$, it yields

$$\dot{V}^{(k)}(x) = (V_x^{(k)})^\top F + (V_x^{(k)})^\top G \hat{u}^{(k+1)}. \quad (32)$$

Since $\hat{H}(x, V^{(k)}, \hat{u}^{(k)}) = 0$, we get

$$(V_x^{(k)})^\top F = -(V_x^{(k)})^\top G \hat{u}^{(k)} - Q(x_1) - \hat{U}_n(\hat{u}^{(k)}, x). \quad (33)$$

By substituting the term $(V_x^{(k)})^\top F$ with (33), (32) becomes

$$\dot{V}^{(k)}(x) = -Q(x_1) - \hat{U}_n(\hat{u}^{(k+1)}, x) - M_t(x), \quad (34)$$

where $M_t(x)$ is

$$M_t(x) = (V_x^{(k)})^\top G(\hat{u}^{(k)} - \hat{u}^{(k+1)}) + \hat{U}_n(\hat{u}^{(k)}, x) - \hat{U}_n(\hat{u}^{(k+1)}, x).$$

It can be deduced from (31) that

$$(V_x^{(k)})^\top G = -2\hat{\lambda}R \tanh^{-1}(\hat{\lambda}^{-1}\hat{u}^{k+1}). \quad (35)$$

Combined with (35) and

$$\begin{aligned} & \hat{U}_n(\hat{u}^k, x) - \hat{U}_n(\hat{u}^{k+1}, x) \\ &= 2 \sum_{i=1}^m \int_{\hat{u}_i^{(k+1)}}^{\hat{u}_i^{(k)}} r_i \hat{\lambda}_i \left(\tanh^{-1}(s/\hat{\lambda}_i) \right) ds, \end{aligned}$$

the term $M_t(x)$ can be rewritten as

$$M_t(x) = 2 \sum_{i=1}^m r_i \hat{\lambda}_i m_i^t,$$

where m_i^t is

$$\begin{aligned} m_i^t &= \int_{\hat{u}_i^{(k+1)}}^{\hat{u}_i^{(k)}} \left(\tanh^{-1}(s/\hat{\lambda}_i) \right) ds \\ &\quad - \tanh^{-1}(\hat{u}_i^{(k+1)}/\hat{\lambda}_i)(\hat{u}_i^{(k)} - \hat{u}_i^{(k+1)}). \end{aligned}$$

Let the function $\beta(s)$ in (27) be $\beta(s) = \tanh^{-1}(s/\hat{\lambda}_i)$ and we have

$$m_i^t = f_\alpha(\hat{u}_i^{(k+1)}, \hat{u}_i^{(k)}) \geq 0,$$

which further implies $M_t(x) \geq 0$.

Since $V^{(k)}(x) \geq 0$ and $V^{(k)}(x) = 0$ if and only if $\|x_1\| = 0$, the function $V^{(k)}(x)$ can be treated as a Lyapunov function for x_1 . Then from (34), we obtain that $\dot{V}^{(k)}(x) \leq 0$ as the functions $Q(x_1)$, $\hat{U}_n(\hat{u}^{(k+1)})$ and $M_t(x)$ are all positive semi-definite. Hence, the x_1 -system can be stabilized by the control policy $\hat{u}^{(k+1)}$. Besides, from (31), it can be observed that $\hat{u}^{(k+1)} = 0$ if $x_1 = 0$. Thus, $\hat{u}^{(k+1)}$ is admissible.

Next, we will prove that $V^*(x) \leq V^{(k+1)}(x) \leq V^{(k)}(x)$. As both $\hat{u}^{(k)}$ and $\hat{u}^{(k+1)}$ are admissible control policies, we have $V^{(k)}(x(t = \infty)) = 0$ and $V^{(k+1)}(x(t = \infty)) = 0$. Taking the derivative of $V^{(k)}(x)$ and $V^{(k+1)}(x)$, respectively, along the trajectory of system $\dot{x} = F(x) + G(x)\hat{u}^{(k+1)}$, it yields

$$\begin{aligned} & V^{(k+1)}(x(t)) - V^{(k)}(x(t)) \\ &= - \int_t^\infty \frac{d(V^{(k+1)}(x) - V^{(k)}(x))}{dx} (F + G\hat{u}^{(k+1)}) d\tau \quad (36) \end{aligned}$$

and

$$\begin{aligned} (V_x^{(k+1)})^\top F &= -(V_x^{(k+1)})^\top G \hat{u}^{(k+1)} - Q(x_1) \\ &\quad - \hat{U}_n(\hat{u}^{(k+1)}). \quad (37) \end{aligned}$$

By substituting (33) and (37) into (36), we derive that

$$\begin{aligned} & V^{(k+1)}(x(t)) - V^{(k)}(x(t)) \\ &= - \int_t^\infty \left[(V_x^{(k)})^\top G(\hat{u}^{(k)} - \hat{u}^{(k+1)}) \right. \\ &\quad \left. + \hat{U}_n(\hat{u}^{(k)}) - \hat{U}_n(\hat{u}^{(k+1)}) \right] d\tau \\ &= - \int_t^\infty M_t(x(\tau)) d\tau \leq 0. \end{aligned}$$

Thus $V^{(k+1)}(x) \leq V^{(k)}(x)$ for $\forall x \in \Omega$. Furthermore, by using the contradiction method, it holds that $V^*(x) \leq V^{(k+1)}(x) \leq V^{(k)}(x)$. ■

Theorem 2 guarantees that the trained control policy is always admissible during the process of policy iteration. Meanwhile, the updated control policy is always better than its previous one. Then to successively solve (30) and (31), the value function $V(x)$ is approximated by a single-layer neural network, which is

$$V(x) = \sum_{j=1}^M w_j^* \sigma_j(x) + \xi(x) = (\mathbf{w}^*)^\top \boldsymbol{\sigma}_M(x) + \xi(x), \quad (38)$$

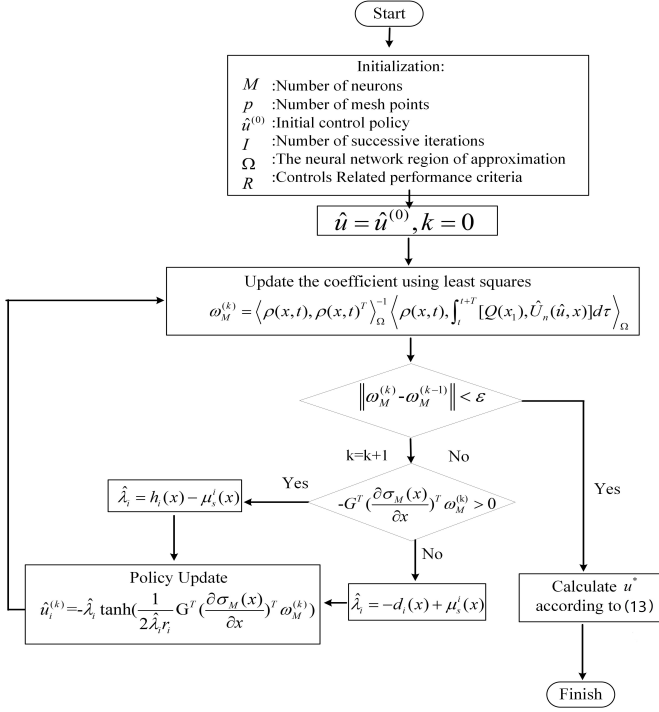


Fig. 1. Flowchart of the proposed IRL algorithm.

where $\sigma_j(x)$ is the activation function and satisfies $\sigma_j(x_1 = 0) = 0$; $\xi(x)$ is the approximation residual error; w_j^* represents the ideal weight of the j -th neuron which minimizes the residual error $\xi(x)$; the vector $\sigma_M(x)$ denotes the vector of activation functions and w^* denotes the ideal weight vector.

Remark 6: It has been pointed out in [6] that the approximation residual error $\xi(x)$ will converge to zero when the number of neurons $M \rightarrow \infty$. Meanwhile, for fixed M , the approximation residual error $\xi(x)$ is also bounded [39]. In practical implementation, the approximation residual error is usually reduced by setting the number of neurons as large as possible. But how to eliminate the approximation residual error $\xi(x)$ completely with a limited number of neurons still requires further investigation.

In order to seek the ideal weight vector w^* , the value function $V^{(k)}(x)$ in the k -th iteration is approximated as

$$V_M^{(k)}(x) = \sum_{j=1}^M w_j^{(k)} \sigma_j(x) = (w_M^{(k)})^\top \sigma_M(x), \quad (39)$$

where $w_j^{(k)}$ and $w_M^{(k)}$ denote the weight of the j -th neuron and the weight vector in the k -th iteration, respectively.

By replacing $V^{(k)}(x)$ in (30) with $V_M^{(k)}(x)$, we have

$$\begin{aligned} (w_M^{(k)})^\top \sigma_M(x(t)) &= \int_t^{t+T} [Q(x_1) + \hat{U}_n(\hat{u}, x)] d\tau \\ &+ (w_M^{(k)})^\top \sigma_M(x(t+T)) - e_M^{(k)}, \end{aligned} \quad (40)$$

where $e_M^{(k)}$ is the residual error defined by

$$\begin{aligned} e_M^{(k)} &= \int_t^{t+T} [Q(x_1) + \hat{U}_n(\hat{u}, x)] d\tau \\ &+ (w_M^{(k)})^\top [\sigma_M(x(t+T)) - \sigma_M(x(t))]. \end{aligned} \quad (41)$$

Obviously, the parameter w_M should be tuned to reduce the residual error. Here we define a to-be-minimized index as

$$S = \int_{\Omega} |e_M^{(k)}(x)|^2 dx.$$

To minimize S , the weights w_M is determined by

$$\left\langle \frac{de_M^{(k)}(x)}{dw_M}, e_M^{(k)}(x) \right\rangle_{\Omega} = 0, \quad (42)$$

where the notation $\langle f(x), g(x) \rangle = \int_{\Omega} f(x)g(x)^\top dx$ denotes the Lebesgue integral. Let $\varrho(x, t) = \sigma_M(x(t+T)) - \sigma_M(x(t))$. By substituting (41) into (42), one has

$$\begin{aligned} &\left\langle \varrho(x, t), \int_t^{t+T} [Q(x_1) + \hat{U}_n(\hat{u}, x)] d\tau \right\rangle_{\Omega} \\ &+ \left\langle \varrho(x, t), \varrho(x, t)^\top \right\rangle_{\Omega} w_M^{(k)} = 0. \end{aligned} \quad (43)$$

To solve $w_M^{(k)}$, we impose the following assumption in the spirit of persistent excitation (PE) condition.

Assumption 2: For all admissible control policies $\mu(x) \in \mathcal{A}(\Omega)$, there exist constants $\bar{m}_c > 0$ and $\gamma_c > 0$ such that

$$\frac{1}{m_c} \sum_{i=1}^{m_c} \varrho(x, t_i) \varrho(x, t_i)^\top \geq \gamma_c I_M \quad (44)$$

for all $m_c \geq \bar{m}_c$.

Let p represent the number of points in the sample set Ω . If Assumption 2 holds and $p \geq \bar{m}_c$, it can be inferred that $\langle \varrho(x, t), \varrho(x, t)^\top \rangle_{\Omega}$ is invertible. Thus, based on (43), $w_M^{(k)}$ is updated as

$$\begin{aligned} w_M^{(k)} &= -\langle \varrho(x, t), \varrho(x, t)^\top \rangle_{\Omega}^{-1} \times \\ &\left\langle \varrho(x, t), \int_t^{t+T} [Q(x_1) + \hat{U}_n(\hat{u}, x)] d\tau \right\rangle_{\Omega}. \end{aligned} \quad (45)$$

Afterwards, in order to solve (45), an iterative algorithm proposed by [6] is adopted. Given some points over the integration region on Ω , define

$$\begin{aligned} L &= [\varrho(x, t)|_{x_1}, \dots, \varrho(x, t)|_{x_p}], \\ Y &= \left[\int_t^{t+T} (Q(x_1) + \hat{U}_n(\hat{u}, x)) d\tau|_{x_1}, \dots, \right. \\ &\left. \int_t^{t+T} (Q(x_1) + \hat{U}_n(\hat{u}, x)) d\tau|_{x_p} \right]. \end{aligned}$$

Then we get

$$\begin{aligned} \langle \varrho(x, t), \varrho(x, t)^\top \rangle_{\Omega} &= \lim_{\|\delta x\| \rightarrow 0} (L^\top L) \delta x \\ \left\langle \varrho(x, t), \int_t^{t+T} [Q(x_1) + \hat{U}_n(\hat{u}, x)] d\tau \right\rangle_{\Omega} &= \lim_{\|\delta x\| \rightarrow 0} (L^\top Y) \delta x. \end{aligned} \quad (46)$$

By using (46), we rewrite (45) as

$$w_M^{(k)} = -(L^\top L)^{-1} (L^\top Y). \quad (47)$$

Remark 7: Assumption 2 is a common assumption in the current study of ADP [7], [11], [40]. Theoretically, the validity of Assumption 2 is related to the integration time T and the richness of the collected samples. It has been pointed out in [14] that if a proper integral time T is selected, the sample size p just needs to be no smaller than M such that the matrix $\langle \varrho(x, t), \varrho(x, t)^\top \rangle_\Omega$ is invertible. However, it still remains an unsolved problem on how to select such a proper integral time T . As a consequence, in practical implementation, to enrich the diversity of samples so that Assumption 2 holds, the control input in the training phase is expected to be persistently exciting, which is usually guaranteed by adding a small exploration noise to the original control input [14]. After the training is finished, the exploration noise is removed. Meanwhile, the size of the sample set Ω is usually chosen as large as possible to guarantee $p \geq m_c$.

According to the definition of $\hat{\lambda}_i$ in (8), the sign of each element $\hat{\mu}_i(x)$ of $\hat{\mu}(x)$ should be evaluated in advance. From the structure of $\hat{\mu}_i(x)$ in (31), it can be found that the sign of $\hat{u}_i(t)$ is the same as that of the i -th element of $-G^\top(x)V_x^{(k)}(x)$. Thus, the matrix $\hat{\lambda}$ can be determined by calculating $-G^\top(x)V_x^{(k)}(x)$ in advance. Specifically, the i -th element of $\hat{\lambda}$ on the diagonal is determined by

$$\hat{\lambda}_i = \begin{cases} h_i(x) - \mu_s^i(x), & \text{if } z_i \geq 0, \\ -d_i(x) + \mu_s^i(x), & \text{if } z_i < 0, \end{cases}$$

where z_i is the i -th element of $-G^\top(x)V_x^{(k)}(x)$.

The iterations is terminated when the error of the coefficients obtained at two consecutive steps is smaller than a given threshold ϵ . The flow chart of the proposed IRL algorithm is presented in Fig. 1.

Remark 8: As the traditional admissible control policies can stabilize the system, the initial control policy $u(t)$ defined by (5) with the NN weight being zero vector is also admissible. Thus in the PI algorithm described above, the NN weight can be initialized as zero vector directly.

III. APPLICATION TO THE OPTIMAL UAV CIRCUMNAVIGATION PROBLEM

In this section, we employ the method proposed in this paper to solve a practical problem: the optimal UAV circumnavigation control problem. As the target's position is usually estimated from the on-board sensor measurement, which often contains noise, a filter like Extended Kalman Filter (EKF) is needed. It has been shown in [41] that the performance of the filter is dependent on the UAV's trajectory. In this section, we intend to design an optimal circumnavigation controller based on the Fisher information, which can quantify the information provided by the sensor measurement [42]. Generally speaking, the more Fisher information the UAV gains, more accurate the estimated target position will be [43]. Specifically, the UAV is controlled to circumnavigate around the target (see Fig. 2), while minimizing an objective function involving Fisher information in the circumnavigation trajectory. A simulation result is presented in which the performance of the control law designed by our method is compared with the method proposed in [20].

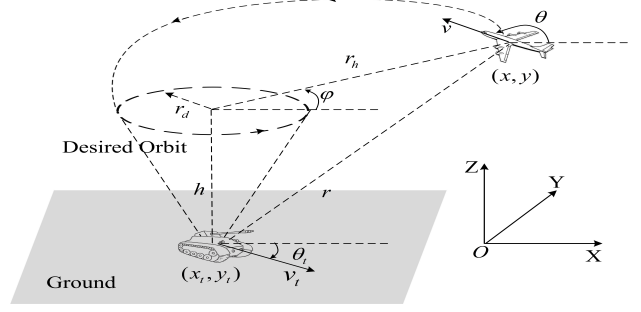


Fig. 2. The illustration of circumnavigation around a ground moving vehicle.

A. Problem formulation of the optimal UAV circumnavigation

Consider a fixed-wing UAV, whose kinematic model is described by

$$\begin{cases} \dot{x}_p = v \cos \theta, \\ \dot{y}_p = v \sin \theta, \\ \dot{\theta} = u_\theta, \\ v = u_v, \end{cases} \quad (48)$$

where (x_p, y_p) is the position of the UAV and θ denotes the heading angle of the UAV; v is the UAV's linear velocity; u_v and u_θ are the control inputs. The height of the UAV is assumed to be held constant. Owing to the roll angle constraint of the fixed-wing UAV, the following unsymmetrical input constraint is enforced on the UAV:

$$-\frac{\omega_{\min}}{1 + 0.02v} \leq u_\theta \leq \frac{\omega_{\max}}{1 + 0.02v},$$

where the constants $\omega_{\max}, \omega_{\min} > 0$ and $\omega_{\max} \neq \omega_{\min}$. It is obvious that the input saturation constraint is unsymmetrical and depends on the UAV's linear velocity. Note that the linear velocity v is not constant but is dependent on the UAV's state, which will be illustrated later.

Let $s_t = (x_t, y_t)^\top \in \mathbb{R}^2$ represent the position of the moving target. It is assumed that the ground target moves with a constant linear velocity v_t and the dynamics of the target is described by

$$\begin{cases} \dot{x}_t = v_t \cos \theta_t, \\ \dot{y}_t = v_t \sin \theta_t, \\ \dot{\theta}_t = h(\theta_t), \end{cases} \quad (49)$$

where θ_t is the heading of the target, and $h(\theta_t)$ is an unknown function.

As the UAV is expected to hold a constant angular speed with a preset circumnavigation radius, the relative speed v_r of the UAV is also expected to be constant. The relative angle of the UAV w.r.t. the target is denoted by θ_r , which satisfies

$$\begin{cases} v_r \cos \theta_r = v \cos \theta - v_t \cos \theta_t, \\ v_r \sin \theta_r = v \sin \theta - v_t \sin \theta_t. \end{cases} \quad (50)$$

The linear speed of the UAV is dependent on the UAV's state and can be obtained from (50) as

$$v = v_t \cos(\theta - \theta_t) + \sqrt{v_t^2 \cos^2(\theta - \theta_t) + v_r^2 - v_t^2}. \quad (51)$$

The UAV is assumed to utilize a radar as the measurement sensor. Let $s_r = (x_r, y_r)^\top = (x_p - x_t, y_p - y_t)^\top$ denote the relative position between the UAV and the target. Then with

the aid of the radar, the UAV can sense the range and bearing information with the observation model described by

$$\zeta(t) = \mathcal{Z}(s_r) + \chi(t),$$

where $\zeta(t)$ is the sensor measurement; $\chi(t)$ is the measurement noise; $\mathcal{Z}(s_r)$ is the observation function defined by

$$\mathcal{Z}(s_r) = \begin{bmatrix} r \\ \varphi \end{bmatrix} = \begin{bmatrix} \sqrt{x_r^2 + y_r^2 + h^2} \\ \arctan(y_r/x_r) \end{bmatrix}, \quad (52)$$

where h is the height of the UAV; r is the distance between the UAV and the target in 3-dimensional space; φ is the bearing angle between the target and the UAV in the plane.

The circumnavigation radius error e_r is defined by

$$e_r = r_h - r_d, \quad (53)$$

and a state η is defined by

$$\eta = \frac{\pi}{2} - (\theta_r - \varphi), \quad (54)$$

where r_d is the desired circumnavigation radius around the target and $r_h = \sqrt{x_r^2 + y_r^2}$ represents the current circumnavigation radius. Note that the desired circumnavigation around the target is achieved if the conditions $e_r = 0$ and $\eta = 0$ are satisfied [44]. Thus, to make the state e_r and η converge to zero, the dynamics of e_r and η will be analyzed first. The dynamics of e_r is

$$\begin{aligned} \dot{e}_r = \dot{r}_h &= \frac{x_r \dot{x}_r + y_r \dot{y}_r}{r_h} = v_r \cos \varphi \cos \theta_r + v_r \sin \varphi \sin \theta_r \\ &= v_r \cos(\varphi - \theta_r) = v_r \sin \eta. \end{aligned} \quad (55)$$

Deriving both sides of the equation (50) by time t , one has

$$\begin{aligned} -v_r \sin \theta_r \dot{\theta}_r &= v_t \sin \theta_t \dot{\theta}_t + \dot{v} \cos \theta - v \sin \theta \dot{\theta}, \\ v_r \cos \theta_r \dot{\theta}_r &= -v_t \cos \theta_t \dot{\theta}_t + \dot{v} \sin \theta + v \cos \theta \dot{\theta}. \end{aligned}$$

By eliminating \dot{v} , it yields

$$\dot{\theta}_r = \frac{v}{v_r \cos(\theta_r - \theta)} \dot{\theta} - \frac{v_t \cos(\theta - \theta_t)}{v_r \cos(\theta_r - \theta)} \dot{\theta}_t. \quad (56)$$

Further, the dynamics of φ can be obtained by

$$\begin{aligned} \dot{\varphi} &= \frac{x_r \dot{y}_r - y_r \dot{x}_r}{r_h^2} = \frac{\cos \varphi (v_r \sin \theta_r) - \sin \varphi (v_r \cos \theta_r)}{r_h} \\ &= \frac{v_r \sin(\theta_r - \varphi)}{r_h} = \frac{v_r \cos \eta}{r_d + e_r}. \end{aligned} \quad (57)$$

By combining (56) and (57), it yields

$$\begin{aligned} \dot{\eta} &= \dot{\varphi} - \dot{\theta}_r \\ &= \frac{v_r \cos \eta}{r_d + e_r} + \frac{v_t \cos(\theta - \theta_t)}{v_r \cos(\theta_r - \theta)} \dot{\theta}_t - \frac{v}{v_r \cos(\theta_r - \theta)} \dot{\theta}, \end{aligned}$$

where θ_r is determined by (50) and can be calculated by

$$\theta_r = \text{atan2}(v \sin \theta - v_t \sin \theta_t, v \cos \theta - v_t \cos \theta_t).$$

Define a state variable $x = (e_r, \eta, \theta, \theta_t)^\top$. Then the x -dynamics is described by

$$\begin{cases} \dot{e}_r = v_r \sin \eta, \\ \dot{\eta} = \frac{v_r \cos \eta}{r_d + e_r} + \frac{v_t \cos(\theta - \theta_t)}{v_r \cos(\theta_r - \theta)} h(\theta_t) - \frac{v}{v_r \cos(\theta_r - \theta)} u_\theta, \\ \dot{\theta} = u_\theta, \\ \dot{\theta}_t = h(\theta_t), \end{cases} \quad (58)$$

where the linear speed v of the UAV is given by (51).

It can be observed that system (58) is a NF system as $\dot{\eta} \neq 0$ when e_r , η and u_θ are all 0. By using the method proposed in Section II-B, the control policy $u_\theta(t)$ is designed as

$$u_\theta(t) = u_s(t) + \hat{u}(t), \quad (59)$$

where $u_s(t)$ is the initial control policy and $\hat{u}(t)$ is the virtual input to be designed. Specifically, we adopt the vector field (VF) method proposed in [20] as the initial admissible control policy $u_s(t)$, which is described by

$$u_s = \begin{cases} -k(\theta - \theta_d), & \text{if } k(\theta_d - \theta) \in [-\frac{\omega_{\min}}{1+0.02v}, \frac{\omega_{\max}}{1+0.02v}], \\ \frac{\omega_{\max}}{1+0.02v}, & \text{if } k(\theta_d - \theta) > \frac{\omega_{\max}}{1+0.02v}, \\ -\frac{\omega_{\min}}{1+0.02v}, & \text{if } k(\theta_d - \theta) < -\frac{\omega_{\min}}{1+0.02v}, \end{cases}$$

where θ_d is determined by

$$\begin{bmatrix} \cos \theta_d \\ \sin \theta_d \end{bmatrix} = \frac{-v_r}{r_h (r_h^2 + r_d^2)} \begin{bmatrix} x_r (r_h^2 - r_d^2) + y_r (2r_d r_h) \\ y_r (r_h^2 - r_d^2) - x_r (2r_d r_h) \end{bmatrix}.$$

By substituting (59) into (58), the x -dynamics becomes

$$\begin{cases} \dot{e}_r = v_r \sin \eta, \\ \dot{\eta} = \frac{v_r \cos \eta}{r_d + e_r} + \frac{v_t \cos(\theta - \theta_t)}{v_r \cos(\theta_r - \theta)} h(\theta_t) - \Lambda u_s - \Lambda \hat{u}, \\ \dot{\theta} = u_s + \hat{u}, \\ \dot{\theta}_t = h(\theta_t). \end{cases} \quad (60)$$

where $\Lambda = v/(v_r \cos(\theta_r - \theta))$ and the virtual input \hat{u} is constrained by

$$u_s - \frac{\omega_{\min}}{1+0.02v} \leq \hat{u} \leq u_s + \frac{\omega_{\max}}{1+0.02v}.$$

Up to now, the system dynamics for the UAV circumnavigation problem has been formulated. Then a to-be-minimized optimization criterion is needed. Firstly, using the method proposed in Section II-B, the control cost function $\hat{U}_n(\hat{u}, x)$ is defined as

$$\hat{U}_n(\hat{u}, x) = 2 \int_0^{\hat{u}} \hat{\lambda} \tanh^{-1}(s/\hat{\lambda}) r ds,$$

where the constant $r > 0$ and $\hat{\lambda} \in \mathbb{R}$ is defined by

$$\hat{\lambda} = \begin{cases} u_s(t) + \frac{\omega_{\max}}{1+0.02v}, & \text{if } \hat{u} \geq 0, \\ u_s(t) - \frac{\omega_{\min}}{1+0.02v}, & \text{if } \hat{u} < 0. \end{cases}$$

Next, a function representing the state cost will be constructed based on the so-called accumulative information [41]. To quantify the utilization of the sensor data, we set up the optimization criterion by exploiting the accumulative information \mathcal{D} based on the Fisher information metric, which is

$$\mathcal{D} = \int_{t_0}^{\infty} \sqrt{L(r_h, \eta)} dt, \quad (61)$$

where $L(r_h, \eta)$ is

$$L(r_h, \eta) = \frac{v_r^2 r_h^2}{r^6 \sigma_r^2} \sin^2 \eta + \frac{8r_h^2 v_r^2}{r^4} \sin^2 \eta + \frac{v_r^2}{r_h^2 \sigma_\varphi^2} \cos^2 \eta; \quad (62)$$

σ_r and σ_φ are two constants representing the standard deviations of the rang and bearing measurements, respectively. The detailed derivation for the formula (62) can be found in our previous work [44].

It can be deduced intuitively from (61) and (62) that the UAV will obtain more accumulative information in the unit time if the circumnavigation radius r_h decreases. In other words, the UAV will fly just above the ground target if one directly takes (61) as a to-be-maximized performance index. However, the UAV is expected to circumnavigate around the target with a given radius, which implies the performance index should reach its extremum at $r_h = r_d$. To achieve this, similar to our previous work [44], a small variation is made based on the definition of the accumulative information and a to-be-minimized performance index is defined as

$$\mathcal{J} = \int_0^\infty \left[(Q_{\max} - \hat{Q}(r_h, \eta)) / Q_{\max} + \hat{U}_n(\hat{u}, x) \right] d\tau, \quad (63)$$

$$\hat{Q}(r_h, \eta) = \sqrt{L(r_h, \eta)} \tanh(r_h - \kappa),$$

where $\hat{Q}(r_h, \eta)$ is a function which varies slightly from the function $\sqrt{L(r_h, \eta)}$; the constant $Q_{\max} = \hat{Q}(r_d, 0)$ equals the value of $\hat{Q}(r_h, \eta)$ when $r_h = r_d$ and $\eta = 0$; κ is a bias constant determined by

$$\frac{d\hat{Q}(r_h, \eta)}{dr_h}(r_h = r_d, \eta = 0) = 0. \quad (64)$$

Specifically, the exact form of (64) can be obtained by

$$\alpha(\kappa) = -\tanh(r_d - \kappa) + r_d(1 - \tanh^2(r_d - \kappa)) = 0.$$

Note that the function $\alpha(\kappa)$ is a monotonically decreasing function and $\kappa < r_d$. Thus the constant κ can be calculated by using the numerical stepwise methods. Affected by the term $\tanh(r_h - \kappa)$, the function $\hat{Q}(r_h, \eta)$ reaches its maximum at $r_h = r_d$ and $\eta = 0$. If the UAV is controlled by the optimal control policy u_θ^* w.r.t. the performance index (63), the desired circumnavigation will be achieved while the accumulative information is maximized [44].

Given system (60) and the performance index (63), the optimal virtual input $\hat{u}^*(t)$ can be obtained through the methods proposed in this paper. Further the optimal control policy $u_\theta^*(t)$ is obtained by $u_\theta^*(t) = u_s(t) + \hat{u}^*(t)$.

B. Simulation result and the comparison with the existing control law

To validate the performance of the designed circumnavigation control law, a numerical simulation is presented in this section. In the simulation, the UAV is expected to circumnavigate around a ground target moving with a linear speed of 5 m/s. The desired circumnavigation radius and the height of the UAV are set as 50 m and 80 m, respectively. The relative linear speed of the UAV w.r.t. the target is 10 m/s. The standard deviation parameters σ_r and σ_φ are assumed to be $\sigma_r = 2 \times 10^{-3}/m$ and $\sigma_\varphi = 1.5 \times 10^{-4}\pi$ rad, respectively. The constants w_{\max} and w_{\min} are set as 1.5 rad/s and 1.2 rad/s, respectively. The function $h(\theta_t)$ which determines the angular speed of the target is appointed as

$$h(\theta_t) = 0.5 - 0.5 \sin^2(\theta_t). \quad (65)$$

In the simulation, the following neural network is utilized to approximate the value function:

$$V_{350}(e_r, \eta, \theta, \theta_t) = \sum_{i=1}^{35} \sum_{j=1}^{10} w_{10(i-1)+j} a_i b_j,$$

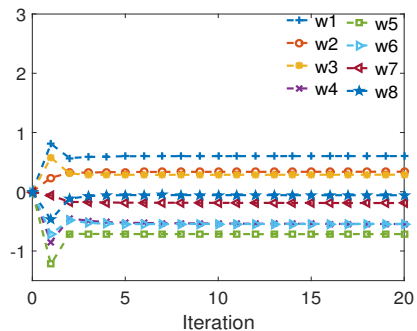


Fig. 3. The convergence of eight representative NN weights.

where a_i and b_j are, respectively, the i -th and j -th elements of the vectors \vec{a} and \vec{b} defined as follows:

$$\begin{aligned} \vec{a} = & [e_r^2, e_r \eta, \eta^2, e_r^4, e_r^3 \eta, e_r^2 \eta^2, e_r \eta^3, \eta^4, e_r^6, e_r^5 \eta, e_r^4 \eta^2, e_r^3 \eta^3, \\ & e_r^2 \eta^4, e_r^5 \eta, \eta^6, e_r^8, e_r^7 \eta, e_r^6 \eta^2, e_r^5 \eta^3, e_r^4 \eta^4, e_r^3 \eta^5, e_r^2 \eta^6, e_r \eta^7, \eta^8, \\ & e_r^{10}, e_r^9 \eta, e_r^8 \eta^2, e_r^7 \eta^3, e_r^6 \eta^4, e_r^5 \eta^5, e_r^4 \eta^6, e_r^3 \eta^7, e_r^2 \eta^8, e_r \eta^9, \eta^{10}]^\top, \\ \vec{b} = & [1, \theta, \theta_t, \theta^2, \theta \theta_t, \theta_t^2, \theta^3, \theta^2 \theta_t, \theta \theta_t^2, \theta_t^3]^\top. \end{aligned}$$

The simulation is conducted with a sample frequency of 200Hz. For each iteration, 40000 samples are collected and used to update the control policy. The convergence of eight representative weights of the neural network is demonstrated in Fig. 3. It can be observed that after 4 iterations, the weights are all nearly convergent. Thus, the stableness and convergence of the proposed IRL-based PI algorithm are verified by Fig. 3.

The trajectories of the ground target and the UAVs controlled by our designed control law are demonstrated in Fig. 4. The variation of the circumnavigation radius r_h controlled by our method is demonstrated in Fig. 6 (red solid line). It is illustrated that the circumnavigation radius r_h converges to the preset radius 50 m. Fig. 5 is the illustration of the variation of the state η controlled by the proposed algorithm during the simulation, which converges to zero at around 17s. The control input of the UAV by our method is illustrated in Fig. 7. Note that the upper bound (blue dash line in Fig. 7) and lower bound (black dash line in Fig. 7) for the control input are changing over time as the speed of the UAV varies. Fig. 7 shows that the control input of the UAV is always within the allowed range during the process of the circumnavigation.

To demonstrate the validity of our method, the proposed control law is further compared with the vector field (VF) guidance law [20]. The comparison of the relative distance r_h between the two methods is demonstrated in Fig. 6. Obviously, the circumnavigation radius controlled by our method converges faster than that of the VF guidance law. Fig. 8 compares the accumulative information of the two methods before the UAV achieves the desired circumnavigation. Note that after achieving the circumnavigation with the desired radius, the UAVs controlled by the two methods gain the same accumulative information in unit time as illustrated in Fig. 9. Therefore, in order to clearly illustrate the difference of the accumulative information obtained by the two methods, Fig. 8

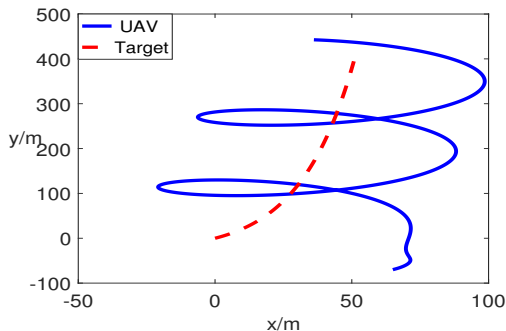


Fig. 4. The illustration of the trajectories of the ground target and the UAV.

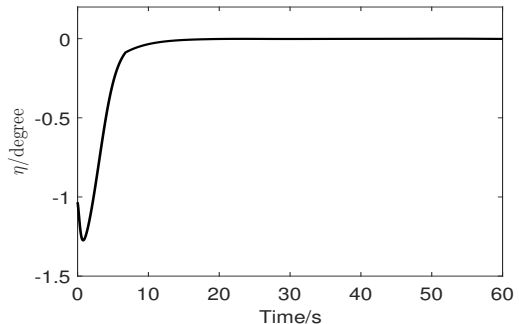


Fig. 5. The variation of η during the circumnavigation.

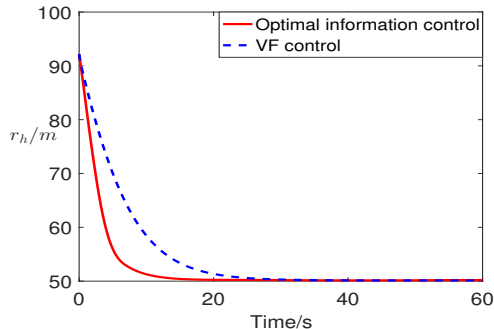


Fig. 6. The variation of the relative distances r_h during the circumnavigation.

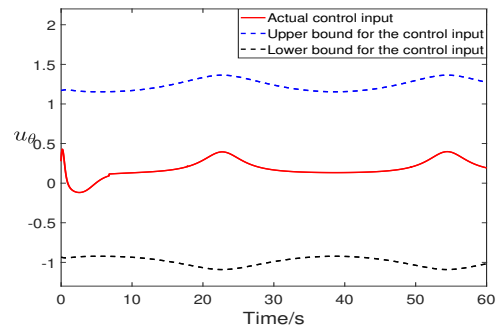


Fig. 7. The variation of the control input.

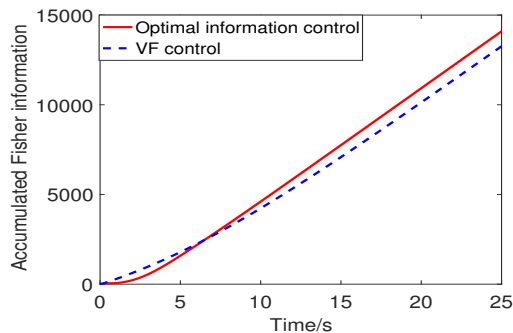


Fig. 8. The variation of the accumulative information during the circumnavigation.

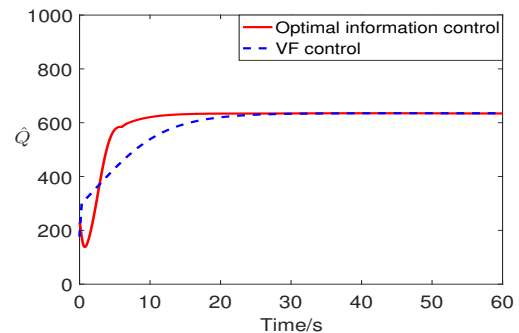


Fig. 9. The variation of \hat{Q} gained per simulation step.

only illustrates the first 25 seconds of the accumulative information. It can be observed from Fig. 8 that the accumulative information acquired by our method is higher than that of the VF method. In order to show this more clearly, we demonstrate the obtained accumulative information per simulation step, i.e., the value of the function $\hat{Q}(r_h, \eta)$, of the two methods in Fig. 9. Overall, the UAV controlled by our method gains more accumulative information before the UAV achieves the desired circumnavigation (except for the first 3 seconds). After the UAV achieves the desired circumnavigation, the values of the function $\hat{Q}(r_h, \eta)$ obtained by the two methods are the same.

IV. CONCLUSIONS

In this paper, we have addressed the optimal control problem for NF nonlinear systems with unsymmetrical and state-dependent input constraint. The method proposed in this paper

relaxes the assumptions on the dynamics and the input constraints of optimal control systems in the existing works. The proposed method is applied to solve an application case: the optimal UAV circumnavigation control problem. The control performance of our algorithm has been compared with the algorithm proposed in [20] by using a numerical simulation.

In the future work, we will extend the proposed optimal control design method to the multi-agent systems and further investigate the optimal cooperative circumnavigation control problem of the multi-UAV systems.

REFERENCES

- [1] J. Vlassenbroeck and R. Van Dooren, "A Chebyshev technique for solving nonlinear optimal control problems," *IEEE Transactions on Automatic Control*, vol. 33, no. 4, pp. 333–340, 1988.
- [2] H. Yang, Q. Hu, H. Dong, and X. Zhao, "ADP-based spacecraft attitude control under actuator misalignment and pointing constraints," *IEEE Transactions on Industrial Electronics*, vol. 69, no. 9, pp. 9342–9352, 2022.

- [3] Y. Deng, T. Liu, and D. Zhao, "Event-triggered output-feedback adaptive tracking control of autonomous underwater vehicles using reinforcement learning," *Applied Ocean Research*, vol. 113, p. 102676, 2021.
- [4] F. L. Lewis, D. Vrabie, and V. L. Syrmos, *Optimal control*. John Wiley & Sons, 2012.
- [5] R. W. Beard, G. N. Saridis, and J. T. Wen, "Approximate solutions to the time-invariant Hamilton–Jacobi–Bellman equation," *Journal of Optimization Theory and Applications*, vol. 96, no. 3, pp. 589–626, 1998.
- [6] M. Abu-Khalaf and F. L. Lewis, "Nearly optimal control laws for nonlinear systems with saturating actuators using a neural network HJB approach," *Automatica*, vol. 41, no. 5, pp. 779–791, 2005.
- [7] T. Bian, Y. Jiang, and Z. Jiang, "Adaptive dynamic programming and optimal control of nonlinear nonaffine systems," *Automatica*, vol. 50, no. 10, pp. 2624–2632, 2014.
- [8] B. Luo, Y. Yang, D. Liu, and H. Wu, "Event-triggered optimal control with performance guarantees using adaptive dynamic programming," *IEEE Transactions on Neural Networks and Learning Systems*, vol. 31, no. 1, pp. 76–88, 2019.
- [9] D. Liu, S. Xue, B. Zhao, B. Luo, and Q. Wei, "Adaptive dynamic programming for control: A survey and recent advances," *IEEE Transactions on Systems, Man, and Cybernetics: Systems*, vol. 51, no. 1, pp. 142–160, 2021.
- [10] H. Jiang and B. Zhou, "Bias-policy iteration based adaptive dynamic programming for unknown continuous-time linear systems," *Automatica*, vol. 136, p. 110058, 2022.
- [11] H. Modares and F. L. Lewis, "Optimal tracking control of nonlinear partially-unknown constrained-input systems using integral reinforcement learning," *Automatica*, vol. 50, no. 7, pp. 1780–1792, 2014.
- [12] D. Wang, D. Liu, H. Li, B. Luo, and H. Ma, "An approximate optimal control approach for robust stabilization of a class of discrete-time nonlinear systems with uncertainties," *IEEE Transactions on Systems, Man, and Cybernetics: Systems*, vol. 46, no. 5, pp. 713–717, 2016.
- [13] K. G. Vamvoudakis, M. F. Miranda, and J. P. Hespanha, "Asymptotically stable adaptive-optimal control algorithm with saturating actuators and relaxed persistence of excitation," *IEEE Transactions on Neural Networks and Learning Systems*, vol. 27, no. 11, pp. 2386–2398, 2015.
- [14] D. Vrabie and F. L. Lewis, "Neural network approach to continuous-time direct adaptive optimal control for partially unknown nonlinear systems," *Neural Networks*, vol. 22, no. 3, pp. 237–246, 2009.
- [15] S. Xue, B. Luo, D. Liu, and Y. Gao, "Event-triggered adp for tracking control of partially unknown constrained uncertain systems," *IEEE Transactions on Cybernetics*, vol. 52, no. 9, pp. 9001–9012, 2022.
- [16] D. Vrabie, O. Pastravanu, M. Abu-Khalaf, and F. L. Lewis, "Adaptive optimal control for continuous-time linear systems based on policy iteration," *Automatica*, vol. 45, no. 2, pp. 477–484, 2009.
- [17] H. Modares, F. L. Lewis, and M. Naghibi-Sistani, "Adaptive optimal control of unknown constrained-input systems using policy iteration and neural networks," *IEEE Transactions on Neural Networks and Learning Systems*, vol. 24, no. 10, pp. 1513–1525, 2013.
- [18] H. Zhang, L. Cui, X. Zhang, and Y. Luo, "Data-driven robust approximate optimal tracking control for unknown general nonlinear systems using adaptive dynamic programming method," *IEEE Transactions on Neural Networks*, vol. 22, no. 12, pp. 2226–2236, 2011.
- [19] Y. Zhang, B. Zhao, and D. Liu, "Deterministic policy gradient adaptive dynamic programming for model-free optimal control," *Neurocomputing*, vol. 387, pp. 40–50, 2020.
- [20] F. Dong, K. You, and J. Zhang, "Flight control for UAV loitering over a ground target with unknown maneuver," *IEEE Transactions on Control Systems Technology*, vol. 28, no. 6, pp. 2461–2473, 2019.
- [21] L. Kong, W. He, Y. Dong, L. Cheng, C. Yang, and Z. Li, "Asymmetric bounded neural control for an uncertain robot by state feedback and output feedback," *IEEE Transactions on Systems, Man, and Cybernetics: Systems*, vol. 51, no. 3, pp. 1735–1746, 2021.
- [22] S. E. Lyshevski, "Optimal control of nonlinear continuous-time systems: design of bounded controllers via generalized nonquadratic functionals," in *Proceedings of the 1998 American Control Conference*, vol. 1, pp. 205–209, IEEE, 1998.
- [23] H. Modares, M. N. Sistani, and F. L. Lewis, "A policy iteration approach to online optimal control of continuous-time constrained-input systems," *ISA Transactions*, vol. 52, no. 5, pp. 611–621, 2013.
- [24] X. Wang, D. Ding, H. Dong, and X.-M. Zhang, "Neural-network-based control for discrete-time nonlinear systems with input saturation under stochastic communication protocol," *IEEE/CAA Journal of Automatica Sinica*, vol. 8, no. 4, pp. 766–778, 2021.
- [25] W. Zhou, H. Liu, H. He, J. Yi, and T. Li, "Neuro-optimal tracking control for continuous stirred tank reactor with input constraints," *IEEE Transactions on Industrial Informatics*, vol. 15, no. 8, pp. 4516–4524, 2018.
- [26] L. Wang, C. L. P. Chen, and H. Li, "Event-triggered adaptive control of saturated nonlinear systems with time-varying partial state constraints," *IEEE Transactions on Cybernetics*, vol. 50, no. 4, pp. 1485–1497, 2020.
- [27] X. Yang and Q. Wei, "Adaptive critic learning for constrained optimal event-triggered control with discounted cost," *IEEE Transactions on Neural Networks and Learning Systems*, vol. 32, no. 1, pp. 91–104, 2021.
- [28] X. Yang and B. Zhao, "Optimal neuro-control strategy for nonlinear systems with asymmetric input constraints," *IEEE/CAA Journal of Automatica Sinica*, vol. 7, no. 2, pp. 575–583, 2020.
- [29] X. Yang and H. He, "Event-driven H_∞ -constrained control using adaptive critic learning," *IEEE Transactions on Cybernetics*, pp. 1–1, 2020.
- [30] Z. Liu, X. Wang, L. Shen, S. Zhao, Y. Cong, J. Li, D. Yin, S. Jia, and X. Xiang, "Mission-oriented miniature fixed-wing UAV swarms: A multilayered and distributed architecture," *IEEE Transactions on Systems, Man, and Cybernetics: Systems*, pp. 1–15, 2020.
- [31] Z. Sun, H. Garcia de Marina, B. D. O. Anderson, and C. Yu, "Collaborative target-tracking control using multiple fixed-wing unmanned aerial vehicles with constant speeds," *Journal of Guidance, Control, and Dynamics*, vol. 44, no. 2, pp. 238–250, 2021.
- [32] I. Shames, S. Dasgupta, B. Fidan, and B. D. O. Anderson, "Circumnavigation using distance measurements under slow drift," *IEEE Transactions on Automatic Control*, vol. 57, no. 4, pp. 889–903, 2011.
- [33] M. Deghat, I. Shames, B. D. O. Anderson, and C. Yu, "Localization and circumnavigation of a slowly moving target using bearing measurements," *IEEE Transactions on Automatic Control*, vol. 59, no. 8, pp. 2182–2188, 2014.
- [34] M. Deghat, E. Davis, T. See, I. Shames, B. D. O. Anderson, and C. Yu, "Target localization and circumnavigation by a non-holonomic robot," in *2012 IEEE/RSJ International Conference on Intelligent Robots and Systems*, pp. 1227–1232, IEEE, 2012.
- [35] J. Sun, J. Yang, W. Zheng, and S. Li, "GPIO-based robust control of nonlinear uncertain systems under time-varying disturbance with application to DC–DC converter," *IEEE Transactions on Circuits and Systems II: Express Briefs*, vol. 63, no. 11, pp. 1074–1078, 2016.
- [36] M. Kumar and S. Mondal, "Recent developments on target tracking problems: A review," *Ocean Engineering*, vol. 236, p. 109558, 2021.
- [37] A. Wei and Y. Wang, "Stabilization and H_∞ control of nonlinear port-controlled hamiltonian systems subject to actuator saturation," *Automatica*, vol. 46, no. 12, pp. 2008–2013, 2010.
- [38] P. Yang, A. Zhang, and D. Zhou, "Event-triggered finite-time formation control for multiple unmanned aerial vehicles with input saturation," *International Journal of Control, Automation and Systems*, vol. 19, no. 5, pp. 1760–1773, 2021.
- [39] K. Hornik, M. Stinchcombe, and H. White, "Universal approximation of an unknown mapping and its derivatives using multilayer feedforward networks," *Neural Networks*, vol. 3, no. 5, pp. 551–560, 1990.
- [40] J. Li, H. Modares, T. Chai, F. L. Lewis, and L. Xie, "Off-policy reinforcement learning for synchronization in multiagent graphical games," *IEEE Transactions on Neural Networks and Learning Systems*, vol. 28, no. 10, pp. 2434–2445, 2017.
- [41] S. Ponda, R. Kolacinski, and E. Frazzoli, "Trajectory optimization for target localization using small unmanned aerial vehicles," in *AIAA Guidance, Navigation, and Control Conference*, p. 6015, IEEE, 2009.
- [42] X. Wang, Y. Cheng, and B. Moran, "Bearings-only tracking analysis via information geometry," in *2010 13th International Conference on Information Fusion*, pp. 1–6, IEEE, 2010.
- [43] L. Chen, R. Cui, J. Gao, and W. Yan, "Cooperative guidance of multiple UAVs for target estimation based on nonlinear model predictive control," in *2016 International Conference on Advanced Robotics and Mechatronics*, pp. 178–183, IEEE, 2016.
- [44] Y. Yu, X. Wang, and L. Shen, "Optimal UAV circumnavigation control with input saturation based on information geometry," *IFAC-PapersOnLine*, vol. 53, no. 2, pp. 2471–2476, 2020.



Yangguang Yu received the B.S., M.S., and Ph.D. degrees from National University of Defense Technology, China, in 2015, 2018, and 2022, respectively. He is currently a Lecturer at College of Intelligence Science and Technology, National University of Defense Technology at Changsha. His research interests include multi-agent systems, unmanned aerial vehicles and optimal adaptive control.



Xiangke Wang (SM'18) received the B.S., M.S., and Ph.D. degrees in Control Science and Engineering from National University of Defense Technology, China, in 2004, 2006 and 2012, respectively. From 2012, he served as a Lecturer, Associate professor and Professor with the College of Intelligence Science and Technology, National University of Defense Technology, China. He was a visiting student at the Research School of Engineering, Australian National University from 2009 to 2011.

His current research interests focus on the control of multi-agent systems and its applications on unmanned aerial vehicles. He has authored or coauthored 2 books and more than 100 publications in peer reviewed journals and international conferences, including IEEE Transactions, IJRNC, CDC, IFAC, ICRA. etc.



Zhiyong Sun received the Ph.D. degree from The Australian National University (ANU), Canberra ACT, Australia, in February 2017. He was a Research Fellow/Lecturer with the Research School of Engineering, ANU, from 2017 to 2018. From June 2018 to January 2020, he worked as a postdoctoral researcher at Department of Automatic Control, Lund University, Lund, Sweden. Since January 2020 he has joined Eindhoven University of Technology (TU/e), the Netherlands, as an assistant professor. His research interests include multi-robotic systems,

control of autonomous formations, distributed control and optimization.



Lincheng Shen received the B.S., M.S., and Ph.D. degrees in automatic control from the National University of Defense Technology, China, in 1986, 1989, and 1994, respectively. In 1989, he joined the Department of Automatic Control, NUDT, where he is currently a full professor and serves as the Dean of the Graduate School. He has been serving as an Editorial Board Member of the Journal of Bionic Engineering since 2007. His research interests include unmanned aerial vehicles, swarm robotics, and artificial intelligence.